INTERACTIONS BETWEEN LIPID MEMBRANES AND DENDRON-GRAFTED SURFACES

By

JIA LI

A thesis submitted to the

School of Graduate Studies

Rutgers, The State University of New Jersey

In partial fulfillment of the requirements

For the degree of

Master of Science

Graduate Program in Chemical and Biochemical Engineering

Written under the direction of

Meenakshi Dutt

And approved by

_____

_____

_____

New Brunswick, New Jersey

October, 2017

ABSTRACT OF THE THESIS

Interactions between lipid membranes and dendron-grafted surfaces

By JIA LI

Thesis Director:

Dr. Meenakshi Dutt

Biofouling is a pervasive problem which demands the creation of smart, antifouling surfaces. Towards this end, we examine the interactions between a dipalmitoylphosphatidylcholine (DPPC) lipid bilayer and a Polyamidoamine (PAMAM) dendron-grafted surface. In addition, we investigate the impact of dendron generation on the system behavior. Our results demonstrate the system dynamics to be determined by the PAMAM dendron generation. To resolve the multiscale dynamical processes occurring over a large spatiotemporal scale, we employ Molecular Dynamics simulations with a coarse-grained implicit solvent force field. The results from our study can be used to guide the design of novel antifouling surfaces which can prevent the adsorption of microorganisms which have lipid membranes.

Acknowledgements

I would like to show my great gratitude to my advisor Dr. Meenakshi Dutt. She has been patient, supportive and encouraging for the past three years. She offered a great deal of expert academic guidance which trained me not only to become a scientist but to think like a scientist. I could not have imaged having a better advisor for my graduate study.

Besides my advisor, I would like to thank Dr. Roth and Dr. Olson for accepting my invitations to join my committee and attend my thesis defense. I also would like to thank my fellow colleagues in Dr. Dutt's research group. It's a pleasure to work with them. Especially thanks to Kai Jin for his excellent help with this project. My sincere thank also goes to Leebyn Chong and Fikret Aydin. They taught me the basics of computational modeling and helped me build up my system. Also I thank Srinivas Mushnoori for his insightful comments and advice. Thanks to Xiaolei Chu and Bin Zhang for their supports.

Finally, I would like to express my deep gratitude to my parents and my spouse for providing me with unfailing support and continuous encouragement throughout my years of study. This achievement would not have been possible without them.

Table of Contents

List of Tables

List of Figures

Chapter 1 Introduction and Objectives

Biofouling can bring risks to a great variety of objects ranging from our daily life to industrial production such as medical devices,[1-4] food packing and storage,[5-8] and marine and industrial equipment.[9-13] Antifouling materials and coatings which can prevent or remove the adsorption of bacteria, proteins or any other organisms on wetted surfaces are of great interest during the past decades.[10, 14] Studies have shown that polymer brushes grafted on supporting substrates can be used as antifouling surfaces or coatings. [15-20] For example, Zhu et.al first presented dendritic surfactant polymers can be served as antifouling materials to diminish the adhesion of platelet.[21] They synthesized maltose dendron by reacting maltonolactone with the peripheral amine groups of the acetal-protected poly(amidoamine) (PAMAM) dendron (G = 2) and used it and hexanal to react with poly(vinlyamine) (PVAm) to obtain the amphiphilic gylcopolymers. The results showed the platelet adhesion was reduced by over 90% when the hydrophobic substrate had these dendritic polymers adsorbed on.

Polyamidoamine (PAMAM) is widely studied because of its dendritic architecture.[22-23] In addition, both experimental[24-28] and computational[29-31] studies have demonstrated PAMAM dendrimers to interact with and penetrate lipid membranes. Lee and Larson[29-30] performed molecular dynamics (MD) simulations of PAMAM dendrimers with the "MARTINI" coarse-grained (CG) force field developed by Marrink et al.[32-33]. They demonstrated the CG models were able to predict experimental results and observed pore formation in dipalmitoylphosphatidylcholine (DPPC) and dimyristoylphosphatidylcholine (DMPC) lipid bilayers induced by PAMAM dendrimers and their dependencies on the

concentration and size of dendrimers. Ma et al. investigated the protonation level of PAMAM dendrimer was determined by its acidity and had great influence on the effective interactions between the dendrimers and cell membranes using the same MARTINI CG force field.[31]

Since a significant fraction of microorganisms encompass lipid bilayers, these findings highlight the potential of PAMAM to serve as an antifouling material. Whereas PAMAM dendrons with carboxylate terminal groups have been grafted onto silica substrate to protect it against the adsorption of heavy metal ions,[34] similar surfaces have yet to be explored for their antifouling properties.

In chapter 2, we introduced implicit solvent coarse-grain molecular dynamics model and use it to simulate DPPC lipid membrane and PAMAM dendron-grafted surface. System components are comprehensively described. The detailed parameterization is provided and justified.

In chapter 3, we report the observations of the dynamics of DPPC lipid membrane interacting with positively charged PAMAM dendron of generations G1 through G5. The lipid membrane can either diffuse towards PAMAM-dendron-grafted surface and develops long term interactions or develop long term interactions with counter ions froze near the top of the simulation box after diffusing towards them. Membrane are more likely to be trapped by G4 and G5 dendrons. The movements of lipid membrane are mostly driven by non-bonded interactions including electrostatics and Van der Waals interactions.

In chapter 4, we make conclusions of our investigation of interactions between DPPC lipid membrane and PAMAM dendron-grafted surface.

Chapter 2 Modeling DPPC lipid membrane and PAMAM dendron-grafted surface using Molecular Dynamics

2.1 Molecular Dynamics and Dry Martini force field

The particle dynamics is resolved by using classical molecular dynamics (MD) simulations.[35-37] MD generates the trajectories of particles by numerically integrating Newton's equations of motion. The forces acting on the beads can be expressed as the gradients of the total potential energy, which encompasses contributions from pair, bond and angle interactions. The Velocity Verlet method is used to integrate the equations of motion because of its greater stability, time reversibility and better preservation of the symplectic form in the phase space over the Euler method.[37] The MD simulations are run using the open source parallelized MD program named LAMMPS. [38]

The implicit-solvent version of CG Martini model, i.e. "Dry" Martini, was first introduced by Arnarez and co-workers.[39] It can enable the resolution of larger spatiotemporal scales by reducing the number of degrees of freedom. It follows the same strategy as the standard Martini[33]: groups four heavy atoms and associated hydrogens into a coarse-grain bead, differentiates from four main types of beads (polar(P), apolar(C), nonpolar(N) and charged(Q)) and eighteen sub-categories depending on the beads' hydrogen-bonding capacities or degrees of polarity. And it uses Lenard-Jones potential for the non-bonded interactions between these CG beads as well. However, it omits the solvent degrees of freedom by reparametrizing the non-bonded interaction matrix of Martini force field to reduce the time and computational resources needed to simulate large systems. Dry Martini can precisely reproduce the general properties of lipid membrane and other substances.[34, 40-42]

2.2 Modeling and Parameterization of the System Components

2.2.1 Lipid membrane

We investigated the dynamics of the interactions between a lipid bilayer membrane and a dendron-grafted surface. To understand the impact of the interactions on the molecular and material properties of the bilayer, we simulated a 29.7 nm × 29.7 nm lipid bilayer. The lipid bilayer encompasses 3200 dipalmitoylphosphatidylcholine (DPPC) molecules.[32-33, 43]. Each lipid molecule has a hydrophilic head group composed of four CG beads and two hydrophobic tails composed of four beads each. Two of the head beads, the choline and the phosphate groups, have opposite charges (+1e and -1e). All parameters of potentials for bonds, angles and non-bonded pairs are taken from the Dry Martini lipid model.[39]

The free-standing lipid bilayer membrane is equilibrated in the canonical ensemble for 100 ns at 330 K. In order to generate a tensionless membrane, the x and y dimensions of the simulation box are varied simultaneously (with corresponding changes to the height of the box to maintain the volume constant). The membrane tension γ is measured by

$$\gamma = \langle L_z \times \left(P_{zz} - 1/2\, P_{xx} - 1/2\, P_{yy}\right) \rangle \qquad (2.1)$$

where L_z is the z dimension of the simulation box, P_{zz} is the normal component of the pressure tensor, and P_{xx} and P_{yy} denote the tangential components of the pressure tensor.[44] We obtain an approximately tensionless membrane whose dimensions are 29.7 nm by 29.7 nm.

2.2.2 Dendron-grafted surface

The Poly(amidoamine) (PAMAM) dendron-grafted surface is modeled at neutral pH.[34, 41] The CG PAMAM dendron is composed of internal tertiary amine junctions, amide

branches, terminal protonated primary amines (+1e) and a short hydrocarbon chain which connects the dendron to the supporting surface.[45] Hydrated chloride counter ions (-1e) are added to maintain the charge neutrality of the system. The dendrons are tethered to a surface composed of uniformly distributed hexagonally close-packed amorphous silica beads.

Table 1. *Details of PAMAM dendron-grafted surfaces of G1 through G5.*

Dendron generation	Number of dendron molecules	Number of protonated terminal amines	Surface coverage
1	900	3600	0.98
2	400	3200	0.96
3	225	3600	0.97
4	100	3200	0.92
5	100	6400	1.00

The PAMAM dendrons are grafted on to an amorphous silica surface so that the neighboring dendron are evenly spaced from each other. The counter ions are distributed uniformly on top of the dendritic brushes to balance the charges and then moved near the upper boundary of the simulation box. The simulation box is set to be 28.2 nm × 28.2 nm in the x and y dimensions, respectively. The dendron-grafted surface system is equilibrated in the canonical ensemble for 100 ns. Due to the highly branched architecture of the dendrons, the crown of each dendron has a non-significant projection over the silica support. The surface coverage is determined by the ratio of the projected area of all dendrons to the total area of the silica surface. When the surface coverage of the PAMAM dendrons over the support is close to full coverage, the dendritic brushes are approximately uniformly distributed over the entire silica support. This allows the membrane to interact

with a homogenous PAMAM-grafted surface, with no vancacies to expose the silica surface to the bilayer. We alter the grafting density for each dendron generation to obtain a fully covered dendron-grafted surface. The details of the PAMAM dendron-grafted surfaces is provided in Table 1.

2.2.3 Combined system parameterization

The DPPC membrane and the PAMAM dendron-grafted surface are placed in a simulation box of dimensions 28.2 nm by 28.2 nm in the x-y plane. The edges of the isolated membrane are trimmed of 454 lipid molecules so that the x- and y- dimensions of the bilayer and dendron-grafted surface are identical. The PAMAM dendron-grafted surface is located at the minimum of the z-dimension of the simulation box with the DPPC membrane placed above it. The z coordinate of the highest dendron bead is the same as the lowest lipid bead to ensure portions of the bilayer and the dendron-grafted surface are within interaction range.

The bonds between the CG beads are represented by harmonic potential

$$E_b = K_b(r - r_0)^2 \tag{2.2}$$

The angles are represented through the cosine squared potential

$$E_a = K_a[\cos(\theta) - \cos(\theta_0)]^2 \tag{2.3}$$

The parameters can be found in earlier studies.[32-34, 41, 43]

The van der Waals component of the non-bonded interactions are modeled by the LJ potential

$$E_{LJ} = 4\varepsilon_{ij}\left(\left(\frac{\sigma_{ij}}{r_{ij}}\right)^{12} - \left(\frac{\sigma_{ij}}{r_{ij}}\right)^{6}\right) \tag{2.4}$$

The parameters ε_{ij} are determined by the categories of the interacting beads and sets the interaction strength. σ_{ij} is the effective bead diameter. The interaction matrix of the explicit solvent MARTINI model is recalibrated in the Dry MARTINI force field to capture the strength of the LJ potentials without the solvent. The electrostatic component of the non-bonded interactions between the charged head groups of the DPPC lipids and the protonated amines is modeled by the Coulombic potential

$$E_C = \frac{C q_i q_j}{\varepsilon r_{ij}} \tag{2.5}$$

where q_i and q_j are charges carried by bead i and j respectively. The relative permittivity is set to 15. Both the non-bonded interaction potentials have cutoffs of 1.2 nm. The LJ potential is shifted smoothly to zero from 0.9 nm to 1.2 nm. The Coulombic potential is shifted smoothly to zero from 0 to 1.2 nm. The neighbor list for each bead (excluding the silica beads) is extended to 1.5 nm and built every time step. The LJ and Coulombic interactions of bonded atoms are turned off. The energy contributions of 1-3 and 1-4 pairs are set to be unaltered. The silica surface beads and counter ions are maintained frozen during the simulations.

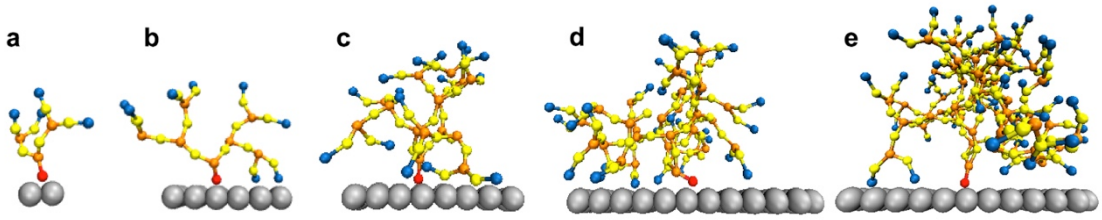

Figure 1. *Simulation snapshot of isolated PAMAM dendron of generations (a) G1, (b) G2, (c) G3, (d) G4 and (e) G5. Silica (silver), termial amine (blue), amide (yellow), internal amine (orange) and hydrocarbon (red) groups are illustrated.*

The z dimension of the simulation box varies from 66.8 nm to 133.7 nm to maintain a counter ion concentration of 0.1 M. The charges carried by the terminal protonated amine

groups are balanced by the chloride ions to preserve the charge neutrality of the system. Since the number of counter ions varies with dendron generation and grafting density, the height of simulation box has to be altered to ensure that the system remains charge neutral and at a constant counter ion concentration. All the counter ions are frozen near the upper boundary of the simulation box. The counter ions are outside the interacting range from both the membrane and dendron-grafted surface. The boundaries are periodic in the x and y dimensions, but not in the z dimension. The top of the simulation box has a fixed Weeks-Chandler-Anderson wall with $\varepsilon = 3.4\text{kJ mol}^{-1}$, $\sigma = 0.47\text{nm}$, and a cut-off distance of 0.528nm.

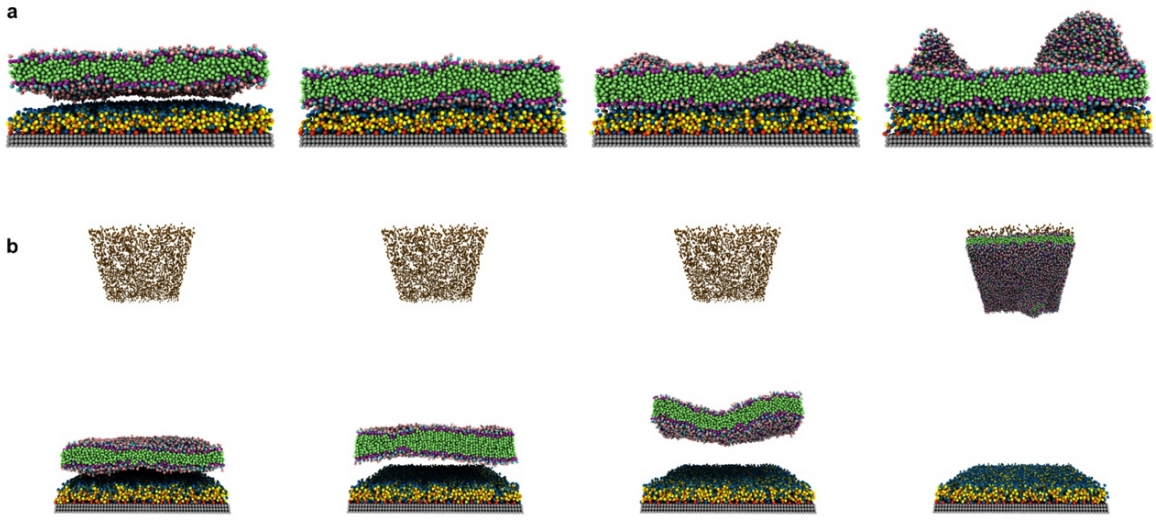

Figure 2. *Simulation snapshots of two outcomes of interactions between tensionless DPPC lipid membrane and PAMAM-dendron-grafted surface: (a) membrane develops sustained interactions with PAMAM dendrons; (b) membrane develops sustained interactions with counter ions, at 0ns, 5ns, 15ns and 100ns from left to right respectively.*

The system is simulated for 100 ns using the canonical ensemble. The temperature of the system is kept at 330 K through the Berendsen thermostat [46]. All simulations are performed using a time step of 10 fs and sampled every 0.1 ns. All results are obtained using ten independent particle trajectories for each dendron generation. The simulations are repeated

for PAMAM dendron generations 1 through 5 (that is, G1, G2, G3, G4 and G5). Figure 1 shows single dendrons of different generations grafted to a surface.

To determine the approximate size of the individual dendrons, we calculated the radius of gyration (R_g) using the following equation

$$R_g^2 = \frac{1}{M}\sum_i m_i \left(r_i - R_{cm}\right) \tag{2.6}$$

M is the total mass of the dendron molecule, R_{cm} is the center-of-mass position, m_i and r_i are the mass and position of a dendron bead. During the span of the simulations, the value of the radius of gyration for each dendron generation has minor fluctuations with time. Hence, the size of the PAMAM dendritic brushes are not affected by the interactions with DPPC membrane.

Chapter 3 Results and Discussion

Our investigations on the interactions between a tensionless DPPC bilayer and PAMAM dendron-grafted surface[34] yield two distinct outcomes. In one outcome, the DPPC membrane diffuses towards the PAMAM dendron-grafted surface to develop long term interactions (Figure 2(a)). In the second outcome, the membrane develops long term interactions with the counter ions after diffusing towards them (Figure 2(b)). The probability of the two outcomes for the different dendron generations is summarized in Figure 3. For surfaces grafted with lower generations of PAMAM dendrons (G1 through G3), both outcomes are equally likely. With increasing generations, the membrane has a greater tendency to develop long-term interactions with the dendron-grafted surface. After developing sustained interactions with either the dendrons or the counter ions, we observe the membrane to gradually bend to form a bowl-shaped configuration. The membrane sustains this configuration while maintaining its structural stability.

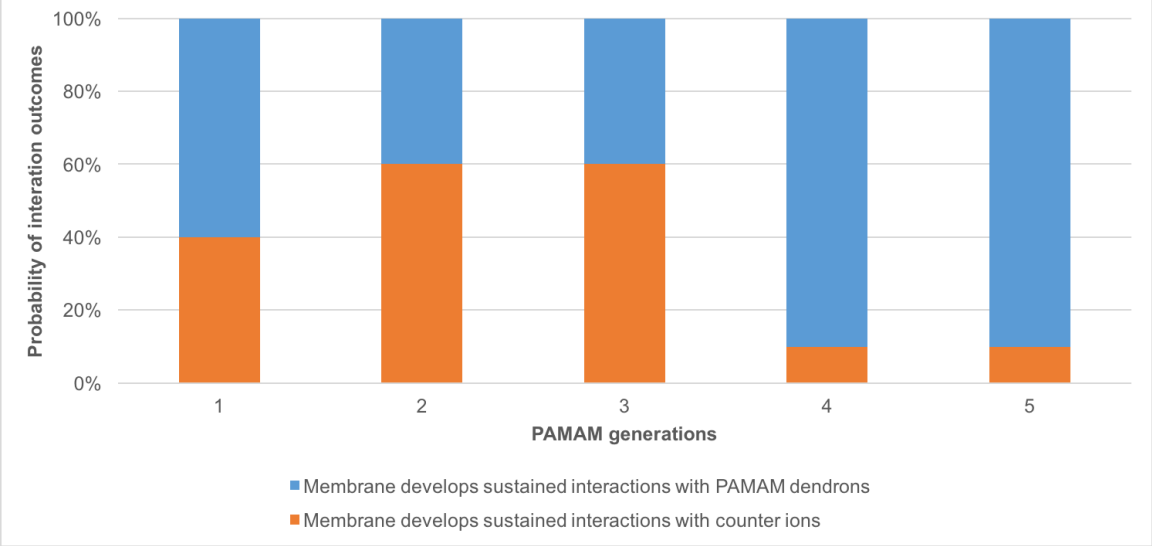

Figure 3. *Probability of interaction outcomes between lipid membrane and PAMAM dendrons for different dendron generations.*

The behavior of the system can be classified into two phases: transient and equilibrium phases. The transient phase encompasses the initial dynamics of the membrane leading to its movement towards the dendrons or the counter ions. The equilibrium phase includes the dynamics of the membrane during its sustained interactions with the dendrons or counter ions, and its bending to form a bowl-shaped configuration. Given the similarity in the results for systems with generations G1 through G3 and G4 through G5, we will be discussing the details of the systems with PAMAM G1 and G5 dendrons.

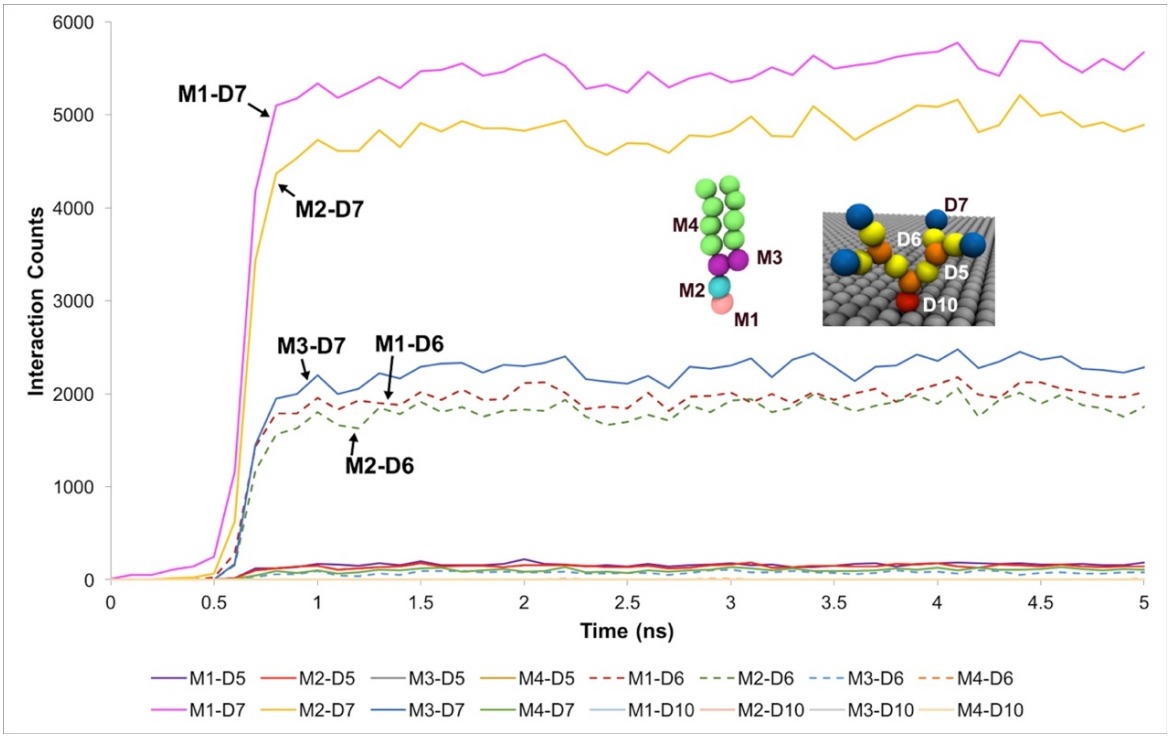

Figure 4. *Interaction counts measurements between different bead types of DPPC lipid and G1 PAMAM dendron when membrane develops long term interactions with dendrons. Labeling of bead types are depicted. Choline (pink), phosphate (cyan), glycerol (purple) and hydrocarbon tail(green) groups of DPPC lipid are labeled as M1, M2, M3 and M4. Terminal amines (blue), amide branches (yellow), internal amines (orange) and tethering hydrocarbon (red) groups of PAMAM dendron are labeled as D7, D6, D5 and D10.*

3.1 Transient Phase

3.1.1 Interaction count

For systems where the membrane develops sustained interactions with the dendrons, the membrane is observed to initially diffuse towards the dendrons. The downwards diffusion activates interactions between the choline moiety of the head groups of the lipids in the membrane and the terminal protonated amines of the dendrons. These interactions coupled with the diffusive motion of the membrane and thermal fluctuations at the molecular scale result cause some of the lipids molecules to further penetrate the dendrons. This penetration leads to two types of interactions. The first one is between the choline and phosphate moieties of the lipid head groups and the amide groups of the dendrons. The second interaction is between the glycerol groups of the lipids and the terminal protonated amines of the dendrons. The lipid head groups are observed to have insignificant interactions with the dendron internal tertiary amine junctions and the short hydrocarbon chain grafting the dendron to the silica surface. The hydrocarbon tails of the phospholipids have some interactions with the PAMAM terminal protonated amines. However, as the number of phospholipid hydrocarbon beads is significantly larger that the lipid head beads, most of the interactions occur between the choline and phosphate moieties of the lipid head groups, and the dendron terminal amines. We surmise that the branched architecture of PAMAM dendrons serves as a barrier to further penetration of the DPPC lipids into the individual dendrons.

These observations are supported by measurements of the interaction counts between the distinct bead types encompass the DPPC membrane and the PAMAM dendrons. Two beads are determined be interacting with each other if their centers of mass are within the interaction range of their pair potentials. Figure 4 summarizes these measurements for a

G1 PAMAM dendron-grafted surface which has long term interactions with the membrane. Most of the interactions occur between the choline moieties of lipids and the terminal protonated primary amines of dendrons, and the phosphate of the phospholipids with the dendron terminal amines. Berényi et al.[26] have reported similar results when studying the effect of G5 PAMAM dendrimers on multilamellar DPPC vesicles. They found PAMAM dendrimers tend to interact with the headgroup region of the lipid bilayers the most according to the Differential Scanning Calorimetry (DSC) measurements. Other significant interactions which are smaller in magnitude include those between the glycerol groups of the lipids and dendron terminal amines, and the choline and phosphate moieties of the lipids with the amide branches of the dendrons. We report similar trends for surface grafted with G2 and G3 PAMAM dendrons which maintain long term interactions with the membrane.

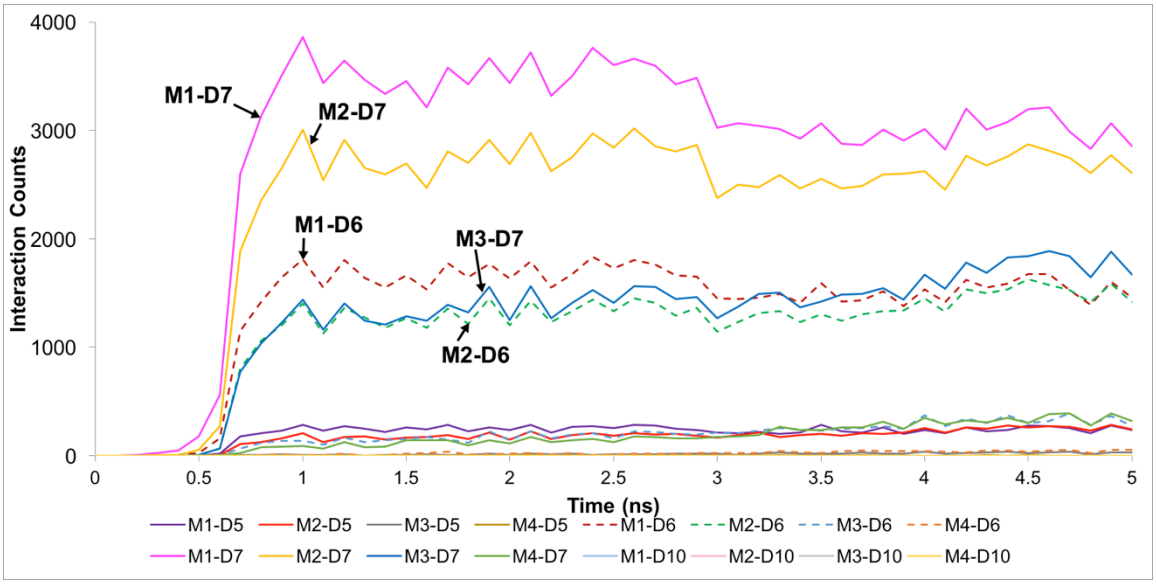

Figure 5. *Interaction counts measurements between different bead types of DPPC lipid and G5 PAMAM dendron when membrane develops long term interactions with dendrons.*

The trends for a G5 PAMAM dendron-grafted surface with long term interactions with a DPPC membrane are similar to those for G1 with some exceptions (see Figure 5). Prior to 3 ns, the interactions between the choline groups of the lipids and the amide branches of

the dendrons are greater than those between the glycerol moieties of the lipids and the dendron terminal protonated amines. This observation is contrary to corresponding results for the G1 surface which demonstrates the interactions between the glycerol groups and the terminal amines to remain consistently greater at all times (in comparison to the choline-amide interactions). In addition, a two-dimensional contour map of the interaction counts of all pairs of bead types between lipids and dendrons at 2 ns shows the G1 dendrons to have spatially uniform interactions with the membrane as compared to its G5 counterpart (see Figure 6). The contour maps can illustrate the interaction counts through the x-y plane and reveal the actual interacting sites of the lipid membrane and PAMAM dendrons. They are obtained by evenly dividing the simulation box into 400 sections along z axis, counting the numbers of interactions in each section. Also, even though each G5 dendron has larger number of beads (in comparison to the G1 dendrons), the number of interactions between the different pairs of beads are consistently lower for the G5 dendrons.

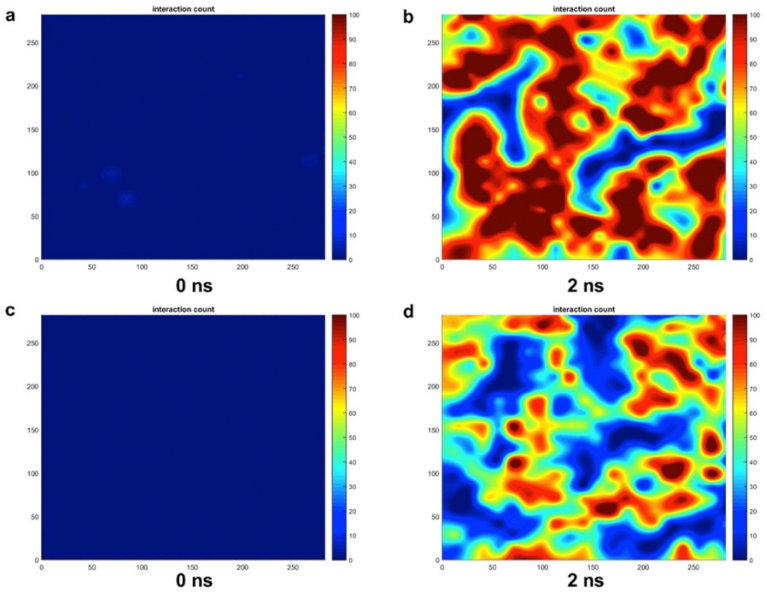

Figure 6. *Two-dimensional contour maps of the interaction count of all pairs of bead types between lipids and (a-b) G1dendrons at 0 ns and 2 ns and (c-d) G5 dendrons at 0 ns and 2 ns when membrane develops long term interactions with dendrons.*

For systems where the membrane diffuses away from the PAMAM dendron-grafted surface to establish sustained interactions with the counter ions, we observe interactions between the lipid and dendrons to occur only at the beginning of the transient phase (see Figure 7). After initial interactions between the choline and phosphate groups with the terminal protonated amines, the membrane moves away until it is outside the interaction range from the dendrons. We examine the role of the electrostatic and van der Waals interactions on the processes underlying the sustained interaction of the membrane with either the counter ions or the dendrons. We focus on the most significant interactions between the membrane and the dendrons (namely, those between the choline and phosphate moieties with the terminal amines).

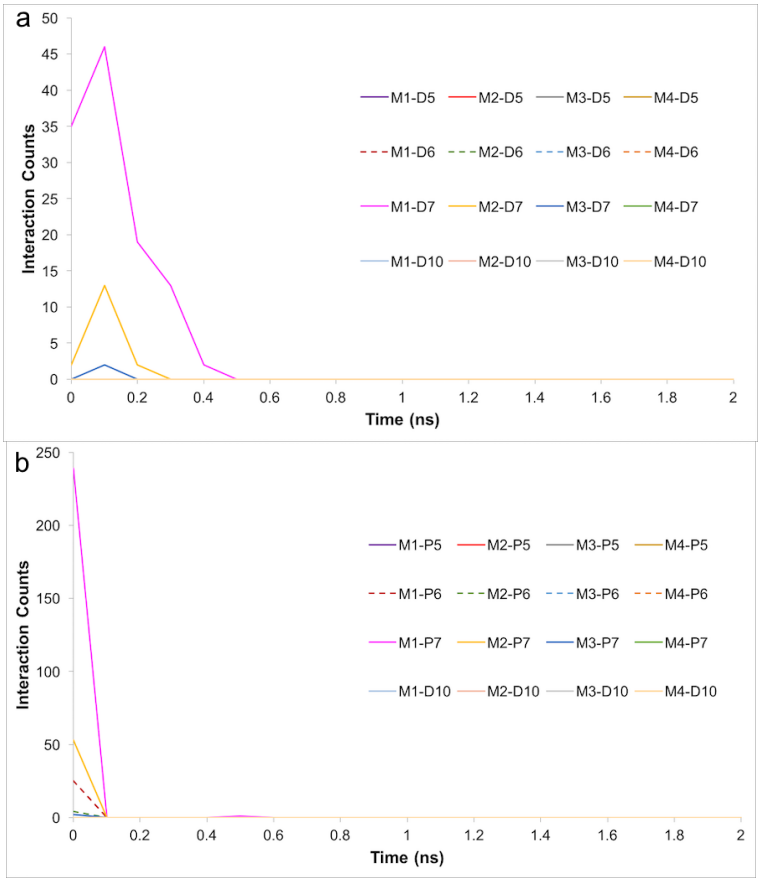

Figure 7*. Interaction count measurements when membrane develops sustained interactions with counter ions of (a) G1 and (b) G5 PAMAM dendron.*

3.1.2 Electrostatic potential energy

We first consider the impact of electrostatic interactions on the process resulting in sustained interactions of the membrane with the PAMAM dendrons, for G1 and G5. The choline and phosphate groups of DPPC carry positive and negative charges, respectively. At neutral pH, the terminal amines of PAMAM are protonated. The electrostatic potential energies between lipid charged head groups and PAMAM terminal pronated amines are provided in Figure 8. The positively charged choline and protonated amines strongly repel each other, as demonstrated by measurements of the corresponding electrostatic potential energy. Whereas the oppositely charged phosphate and terminal protonated amines attract each other strongly. When we combine the effects of electrostatic attraction and repulsion, we find that the electrostatic attraction dominates. Hence, the membrane moves towards the PAMAM dendrons to develop sustained interactions due to the attraction between the oppositely charged phosphate and terminal protonated amines. Based upon the measurements of the electrostatic potentials, the electrostatic repulsion is relatively strong at the early stage of transient phase but gradually decreases. After a few nanoseconds, the electrostatic attraction between the choline and protonated amine moieties begins to dominate.

For the situation when the membrane develops sustained interactions with the counter ions, the repulsive interactions between the choline and protonated amine groups dominate the electrostatic interactions during the initial transient phase. However, the repulsion decreases as the membrane moves away from the dendrons until they are outside the interaction range from each other (see Figure 9).

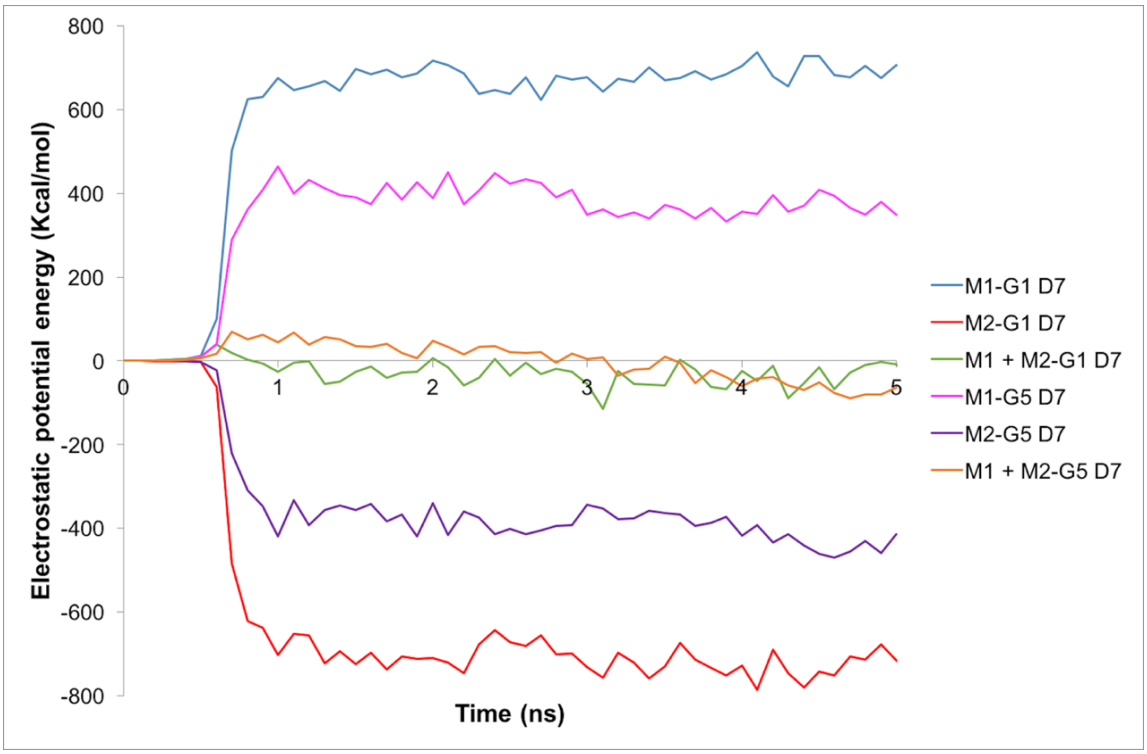

Figure 8. *Electrostatic potential energy measurements for DPPC lipid and G1 and G5 PAMAM dendron when membrane develop sustained interactions with dendrons*.

3.1.3 Van der Waals potential energy

We examine the impact of the van der Waals interactions between different pairs of bead types on the processes underlying the different outcomes, for PAMAM G1 and G5 dendrons. For processes leading to sustained interactions between the membrane and the dendrons, the van der Waals interaction energies between the choline and phosphate groups with the terminal amines are attractive and the most significant. For G1 dendrons as shown in Figure 10(a), the strength of van der Waals potential energy between the phosphate and terminal amine moieties is almost twice as large as those between the choline and terminal amine groups. The difference in these energies is not as significant for G5 dendrons (see Figure 10(b)). The total van der Waals potential energy for the G1 dendron system is approximately ten times larger than that corresponding to G5. This difference arises from the relatively smaller total number of interacting beads in the G5 system. The favorable

van der Waals interactions between the lipid and dendrons further drives the membrane towards the dendron-grafted surface, thereby enabling the development of sustained interactions with both the G1 and G5 dendrons. For the scenario where the membrane developed sustained interactions with the counter ions, the beginning of the transient phase is accompanied by weak van der Waals interactions between the membrane and the dendrons (both G1 and G5). Thereafter, the van der Waals interactions reduce to zero as the membrane moves away from the dendrons.

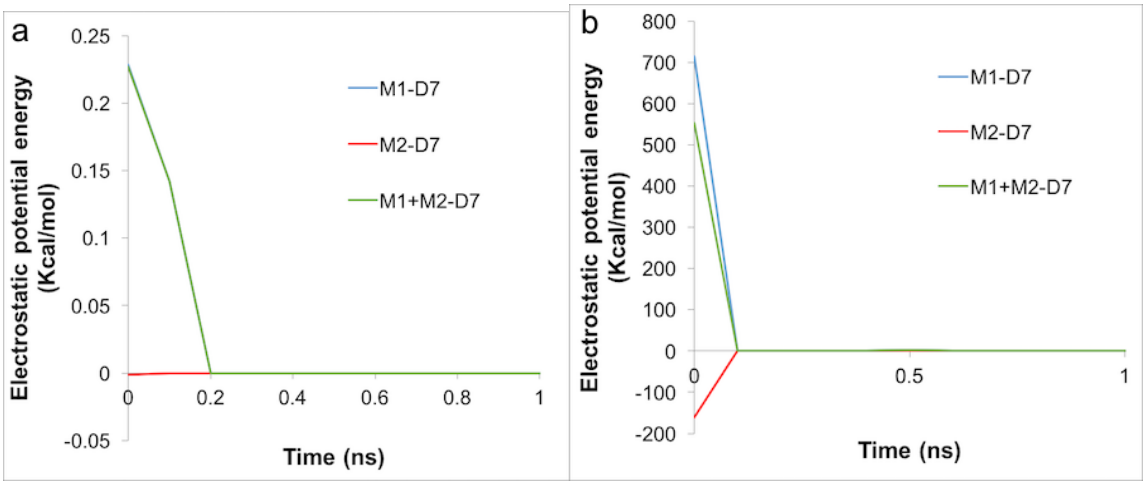

Figure 9. *Electrostatic potential energy measurements when membrane develop sustained interactions with counter ions of (a) G1 and (b) G5 PAMAM dendron.*

3.1.4 Total pair potential energy

To understand the role of the total pair potential on the sequence of processes determining the outcomes for G1 and G5, we combine the electrostatic and van der Waals potential energies between the membrane and the dendrons (see Figure 11). For processes resulting in sustained interactions between the membrane and the dendrons, the electrostatic interactions are initially repulsive. As the charged beads are within the interaction range, the van der Waals interactions begin to increase in strength. During this process, thermal fluctuations can result in the oppositely charged moieties coming within

interaction range from each other. This causes the favorable contributions to the electrostatic and van der Waals potential energies. As more oppositely charged moieties begin to interact, both the electrostatic and van der Waals interactions become increasingly favorable. This sequence of processes drives the membrane to move towards the dendron-grafted surface and develop sustained interactions with it. There are significantly larger fluctuations in the van der Waals potential energy for the G1 dendrons as compared to the G5 dendrons. The difference in the magnitude of the fluctuations arises due to a much higher number of interactions between the G1 dendrons with the membrane. The higher density of interactions increases the sensitivity to minor fluctuations at the molecular scale.

For outcomes where the membrane develops sustained interactions with the counter ions, the transient phase begins with repulsive electrostatic interactions between the membrane and the dendrons (see Figure 12). For the G1 dendrons, the effect of the van der Waals interactions is weak. The dynamics of the molecules do not cause the oppositely charged moieties in the membrane and dendrons to come within interaction range. Hence, the repulsive electrostatic cause the membrane to move away from the dendrons, and eventually develop sustained interactions with the counter ions.

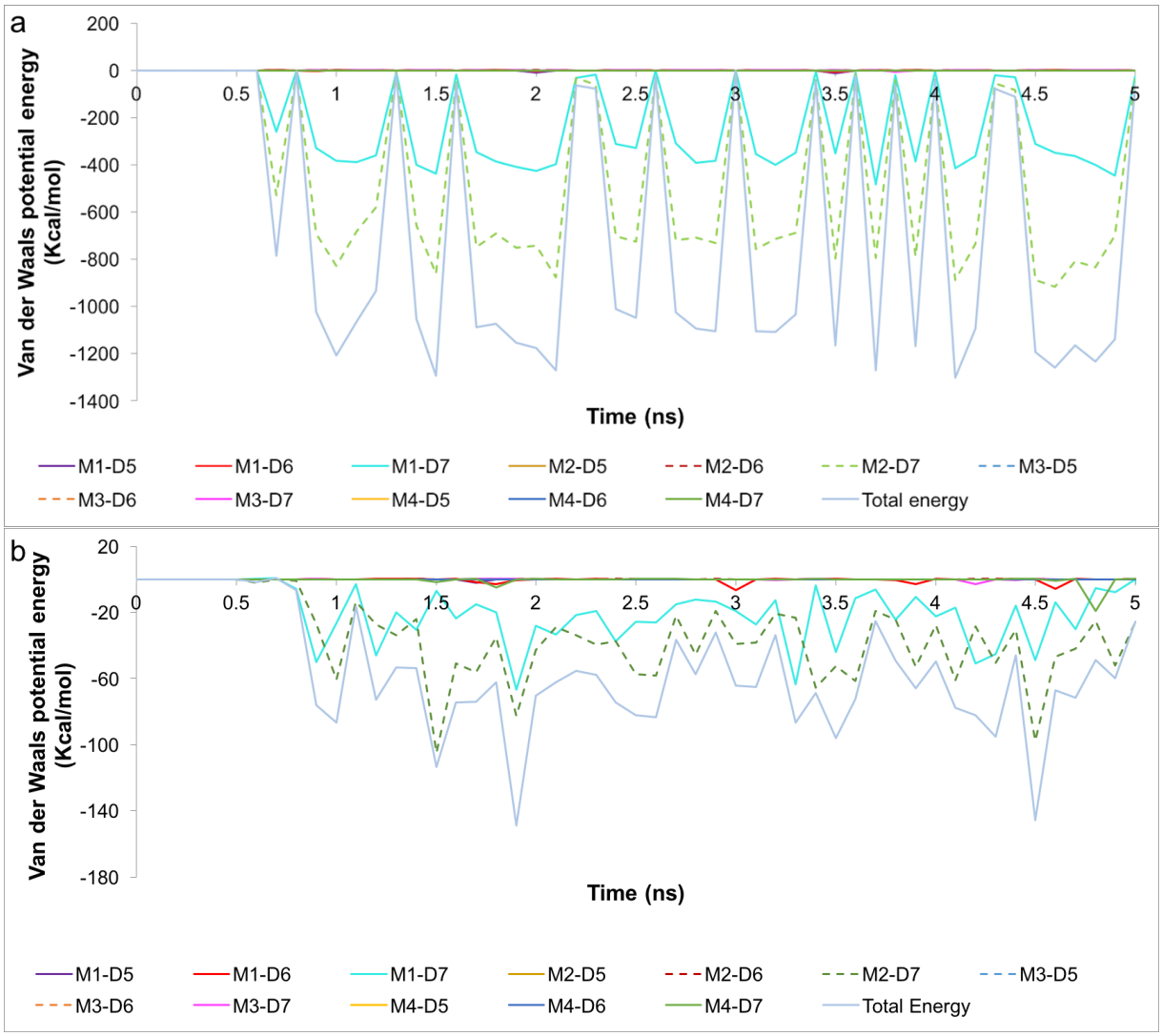

Figure 10. *Van der Waals potential energy measurements when membrane develops sustained interactions with (a) G1and (b) G5 PAMAM dendron.*

We measured the z-component of the average force acting on the DPPC membrane (see Figure 13). For a system which eventually developed sustained interactions with the dendrons, the membrane experiences a relatively strong net force towards the direction of PAMAM dendrons. This is accompanied by a significant increase in the interaction counts. Similarly, a membrane which develops sustained interactions with the counter ions experiences a net positive force (that is, away from the dendron-grafted surface). As there is no force to keep the membrane within interaction range of the dendron, the inertia of the

membrane causes it to move towards the counter ions. Eventually the membrane develops sustained interactions with the counter ions.

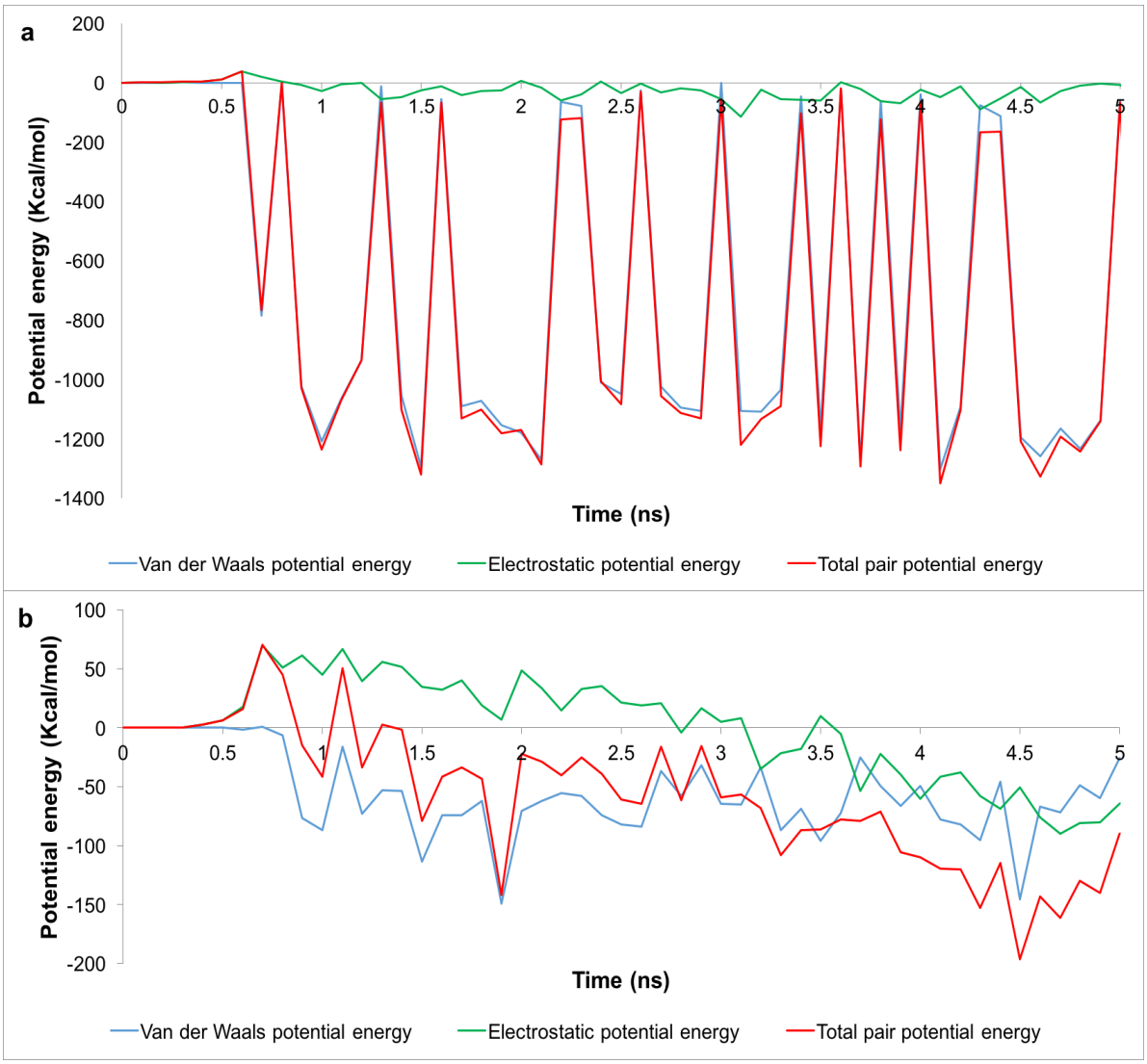

Figure 11. *Potential energy measurements when membrane develops sustained interactions with (a) G1 and (b) G5 PAMAM dendrons.*

For higher dendorn generations (G4 and G5), we observe significant larger numbers of cases of membrane developed sustained interaction with dendrons. The reason that causes this phenomenon could be the difference in architecture of dendron generations. Electronic repulsions of pronated terminal amines cause the branches of each dendron reach out and spread away. The dendrons of higher generations have more terminal groups than lower

ones. It leaves more space between the branches for lipid molecules to penetrate. With the penetration goes on, more phosphate groups fall into the interacting range of the terminal amines. Attractions between oppositely charged moieties along with the attractive van der Waals interactions between the different moieties drag the membrane towards the dendrons and make it difficult for thermal fluctuation to separate them. However, for the lower generation dendrons, their dendritic brushes are more closely packed. The tightly packed dendrons facilitates electrostatic interactions between the electrostatic interactions between the protonated amines and the charged groups of the lipids. Due to insufficient space between the terminal groups, the phospholipids are unable to penetrate the dendrons. Hence if repulsive electrostatic interactions are dominant between the dendrons and the lipids, thermal fluctuations can induce molecular motion which causes the lipids to move away from the dendrons and escape the interaction cutoff range.

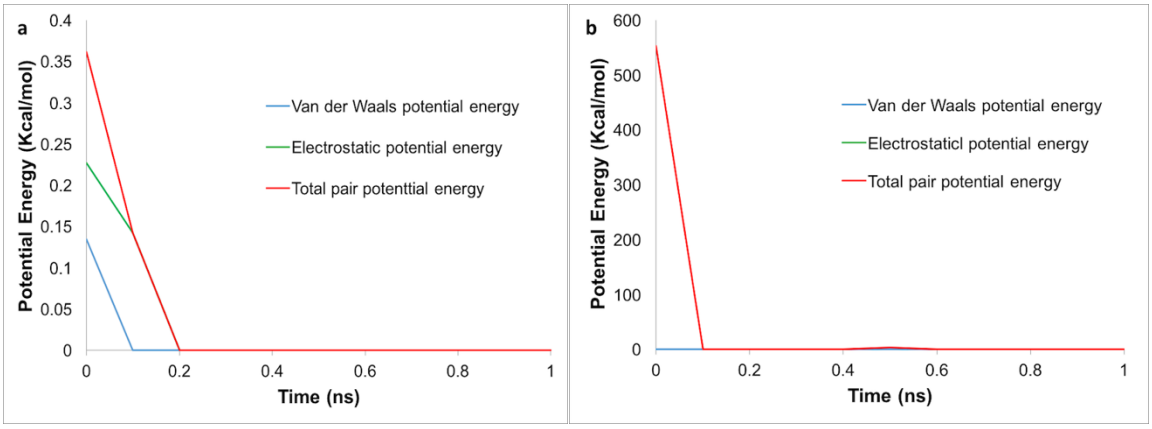

Figure 12. *Potential energy measurements when membrane develops sustained interactions with counter ions of (a) G1and (b) G5 PAMAM dendron.*

Another scenario is that the initial electrostatic repulsion between the lipids and the dendrons are sufficiently strong to push the lipids away from the interaction range from the dendrons. The membrane can only bounce on top of them. Without much driving force

towards the dendrons, the membrane can be kicked away by thermal fluctuation more easily than with dendrons of higher generations.

For the situation where the membrane develops sustained interactions with the dendrons, the initial electrostatic interactions between the lipids and the dendron terminal groups may cause the attractive interactions between the charged moieties to become dominant. With the possible aid of thermal fluctuations, the dendrons to assume configurations where the adjacent protonated amines are sufficiently separated from each other so that the lipids can penetrate the dendrons. which provide space between the terminal groups. The sequence of processes thereafter is similar to what is observed for the higher generation dendrons.

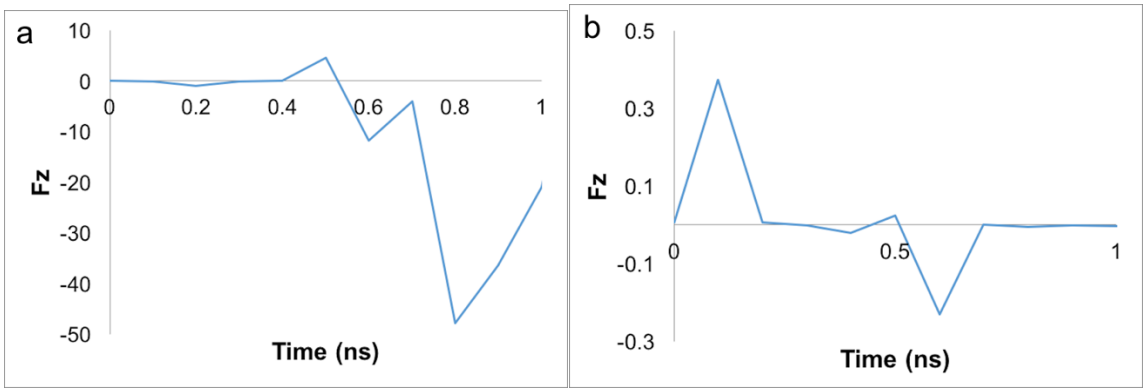

Figure 13. Z-component average force acting on DPPC membrane when membrane develops sustained interactions with (a) G1 PAMAM dendorn and (b) counter ions of G1 PAMAM dendron.

3.2 Equilibrium State

The system attains equilibrium as the membrane moves towards the dendrons or the counter ions. The net charge of the dendrons or the counter ions induces asymmetric stresses across the bilayer. The charged moieties in the lipid head groups are attracted to the oppositely charged groups in the dendrons (or counter ions). The electrostatic attraction leads to changes in the molecular packing on the lipids in the monolayer facing the

dendrons (or counter ions). These molecular scale changes result in asymmetric stresses between the lipid monolayers. This stress is released through the development of excess area in one of the monolayers. Since the two leaflets are coupled to form a stable bilayer, the membrane bends to form a bowl-shaped configuration. The bowl-shaped configuration remains stable through the remainder of the simulation. The curved surface of the bowl is observed to be opposite to the dendrons (or counter ions). During this process, the membrane remains structurally stable and does not rupture.

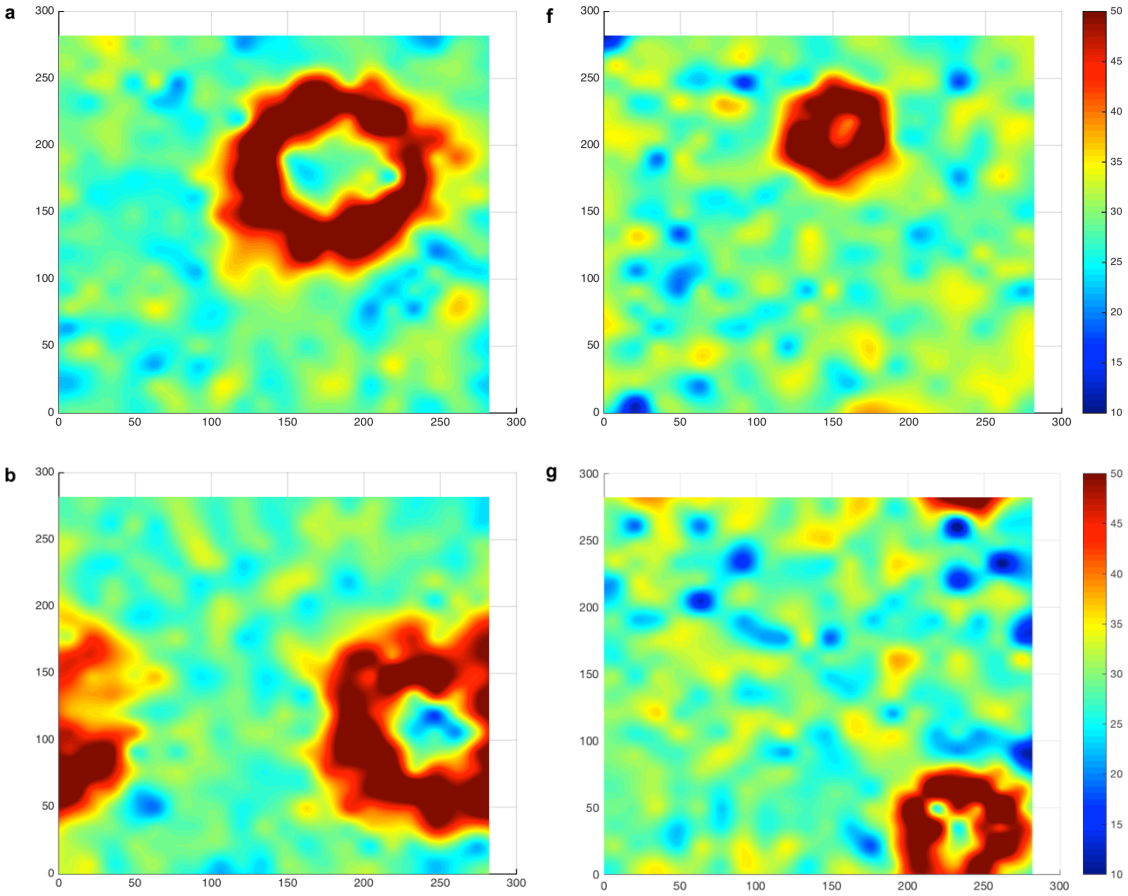

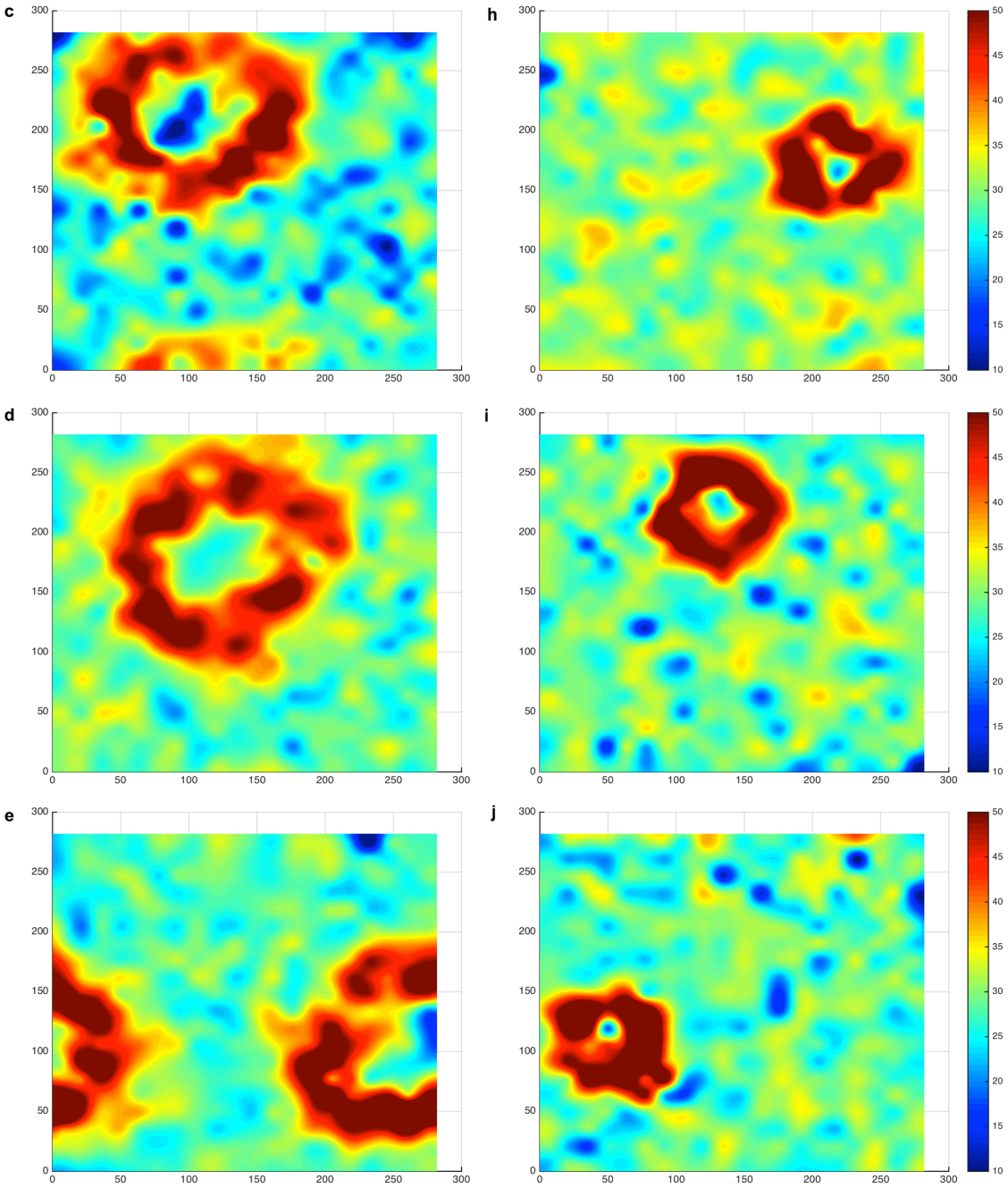

Figure 14. *Two dimensional contour maps of membrane thickness for (a-e) membrane interacts with dendrons and (f-j) membrane interacts with counter ions of G1 through G5 PAMAM dendrons*.

We quantify the deformation of the membrane by measuring its thickness during its interactions with the dendrons (or counter ions). The thickness is determined through the differences in the height of glycerol beads with approximately the same x- and y-

coordinates on the top and bottom membrane leaflets (see Figure 14). The edge of the bowl in a membrane is captured by the dark red circle which indicates that the thickness values of that region is notably higher than the other parts of the membrane. The diameter of the bowls formed for membranes near the dendrons are significantly larger than those formed near the counter ions (see Figure 15). In addition, the diameter of the bowls is observed to typically increase with the PAMAM generation. This can be explained by the excess area induced in the monolayer facing the dendrons or the counter ions. The terminal protonated amines are concentrated in a smaller volume than the counter ions. In addition, the grafting density of dendrons is decreased with dendron generation in order to maintain the consistency of surface coverage. The numbers of dendron molecules of G4 and G5 PAMAM dendron-grafted surfaces are only one ninth of G1 as shown in Table 1. The interacting sites which are the top of the dendritic brushes are distributed more dispersed from G1 through G5. Hence, dendrons with higher generations will induced larger asymmetric stresses and thereby, higher excess area than counter ions in the same system. A membrane with a larger excess area will form a bowl-shape configuration with a larger diameter.

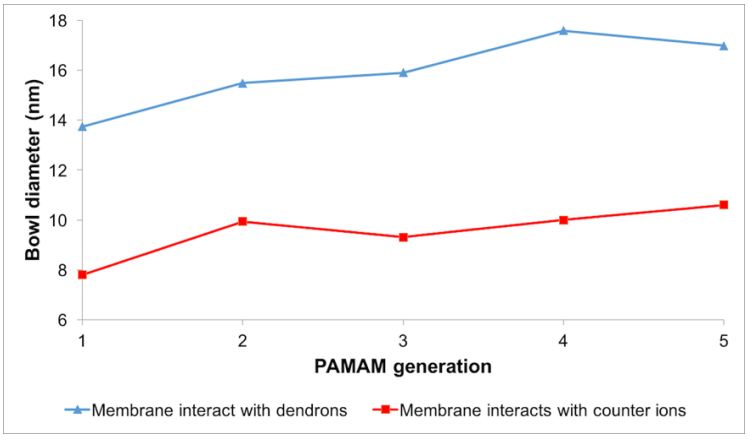

Figure 15. *Bowl size measurements when membrane interacts with dendrons and counter ions of different dendron generations.*

Chapter 4 Conclusions

Studies on interactions between DPPC lipid bilayer and PAMAM dendron-grafted surface were carried by utilizing a coarse-grained implicit solvent MD technique. We examined distinct dynamics of the membrane with PAMAM dendrons of G1 through G5 by analyzing the number of interactions, non-bonded potential energies and the alterations of membrane morphology. Our study reported two outcomes were yield when lipid membrane interacted with PAMAM dendron-grafted surface: membrane moved towards dendrons to develop long term interactions or membrane diffused away from dendrons then developed long term interactions with the counter ions froze near the top of the simulation box. Most interactions happened between charged head groups of lipids and dendron pronated terminal amines. Both electrostatic and Van deer Waals interactions played important roles in the process of attracting membrane to the dendron-grafted surface. The membrane was more likely to be trapped by PAMAM dendron of higher generations (G4 and G5) due to the penetration of membrane led by larger spacing between dendron branches. The lipid membrane deformed into bowl-like configuration after engaging in interactions with either dendrons or counter ions while maintaining its structural stability. This was caused by asymmetric stresses between membrane monolayers introduced by attractions of dendrons. Dendron generations and density of interaction sites can affect the size of the bowl.

As reported in an earlier work, PAMAM dendrimers are capabile of disrupting the multilamellar structure of DPPC membrane.[26] Since bending is observed while membrane interacts with PAMAM dendrons in our study, it is possible for a large cell membrane to

be destructed by dendron-grafted surface due to the asymmetrical stretching. Our investigations can be used to design antifouling surface which can prevent adsorptions of bacteria and other organisms bounded by lipid membrane. The distinct dynamics of lipid membrane with PAMAM dendron of different generations can provide guidance for compositions to achieve the optimal results of repelling bio-attachment. This study can be extended by investigating the interactions dependence on pH and dendron grafting densities. PAMAM dendrons can be replaced by other linear or hyper-branched polymers for more approaches in the antifouling surface area.

Biography

1. Jia Li, K. J., Srinivas Mushnoori, Meenakshi Dutt, Interactions between DPPC lipid membrane and PAMAM dendron-grafted surface. *submitted* **2017**.
2. Donlan, R. M.; Costerton, J. W., Biofilms: survival mechanisms of clinically relevant microorganisms. *Clinical microbiology reviews* **2002,** *15* (2), 167-193.
3. Pavithra, D.; Doble, M., Biofilm formation, bacterial adhesion and host response on polymeric implants—issues and prevention. *Biomedical Materials* **2008,** *3* (3), 034003.
4. Cole, N.; Hume, E. B.; Vijay, A. K.; Sankaridurg, P.; Kumar, N.; Willcox, M. D., In vivo performance of melimine as an antimicrobial coating for contact lenses in models of CLARE and CLPU. *Investigative ophthalmology & visual science* **2010,** *51* (1), 390-395.
5. Meyer, B., Approaches to prevention, removal and killing of biofilms. *International Biodeterioration & Biodegradation* **2003,** *51* (4), 249-253.
6. Li, X.; Xing, Y.; Jiang, Y.; Ding, Y.; Li, W., Antimicrobial activities of ZnO powder-coated PVC film to inactivate food pathogens. *International journal of food science & technology* **2009,** *44* (11), 2161-2168.
7. Conte, A.; Buonocore, G.; Bevilacqua, A.; Sinigaglia, M.; Del Nobile, M., Immobilization of lysozyme on polyvinylalcohol films for active packaging applications. *Journal of food protection* **2006,** *69* (4), 866-870.
8. Kenawy, E.-R.; Worley, S.; Broughton, R., The chemistry and applications of antimicrobial polymers: a state-of-the-art review. *Biomacromolecules* **2007,** *8* (5), 1359-1384.
9. Asuri, P.; Karajanagi, S. S.; Kane, R. S.; Dordick, J. S., Polymer–nanotube–enzyme composites as active antifouling films. *Small* **2007,** *3* (1), 50-53.
10. Yebra, D. M.; Kiil, S.; Dam-Johansen, K., Antifouling technology—past, present and future steps towards efficient and environmentally friendly antifouling coatings. *Progress in organic Coatings* **2004,** *50* (2), 75-104.
11. Chambers, L. D.; Stokes, K. R.; Walsh, F. C.; Wood, R. J., Modern approaches to marine antifouling coatings. *Surface and Coatings Technology* **2006,** *201* (6), 3642-3652.
12. Flemming, H.-C., Biofouling in water systems–cases, causes and countermeasures. *Applied microbiology and biotechnology* **2002,** *59* (6), 629-640.
13. Almeida, E.; Diamantino, T. C.; de Sousa, O., Marine paints: the particular case of antifouling paints. *Progress in Organic Coatings* **2007,** *59* (1), 2-20.
14. Rascio, V. J., Antifouling coatings: where do we go from here. *Corrosion Reviews* **2000,** *18* (2-3), 133-154.
15. Glinel, K.; Jonas, A. M.; Jouenne, T.; Leprince, J.; Galas, L.; Huck, W. T., Antibacterial and antifouling polymer brushes incorporating antimicrobial peptide. *Bioconjugate chemistry* **2008,** *20* (1), 71-77.
16. Fan, X.; Lin, L.; Messersmith, P. B., Cell fouling resistance of polymer brushes grafted from Ti substrates by surface-initiated polymerization: effect of ethylene glycol side chain length. *Biomacromolecules* **2006,** *7* (8), 2443-2448.
17. Wang, B.; Jin, T.; Han, Y.; Shen, C.; Li, Q.; Lin, Q.; Chen, H., Bio-inspired terpolymers containing dopamine, cations and MPC: a versatile platform to construct a

recycle antibacterial and antifouling surface. *Journal of Materials Chemistry B* **2015,** *3* (27), 5501-5510.
18. Kuroki, H.; Tokarev, I.; Nykypanchuk, D.; Zhulina, E.; Minko, S., Stimuli-Responsive Materials with Self-Healing Antifouling Surface via 3D Polymer Grafting. *Advanced Functional Materials* **2013,** *23* (36), 4593-4600.
19. Lau, K. H. A.; Ren, C.; Sileika, T. S.; Park, S. H.; Szleifer, I.; Messersmith, P. B., Surface-grafted polysarcosine as a peptoid antifouling polymer brush. *Langmuir* **2012,** *28* (46), 16099-16107.
20. Yang, C.; Ding, X.; Ono, R. J.; Lee, H.; Hsu, L. Y.; Tong, Y. W.; Hedrick, J.; Yang, Y. Y., Brush-Like Polycarbonates Containing Dopamine, Cations, and PEG Providing a Broad-Spectrum, Antibacterial, and Antifouling Surface via One-Step Coating. *Advanced Materials* **2014,** *26* (43), 7346-7351.
21. Zhu, J.; Marchant, R. E., Dendritic saccharide surfactant polymers as antifouling interface materials to reduce platelet adhesion. *Biomacromolecules* **2006,** *7* (4), 1036-1041.
22. Esfand, R.; Tomalia, D. A., Poly (amidoamine)(PAMAM) dendrimers: from biomimicry to drug delivery and biomedical applications. *Drug discovery today* **2001,** *6* (8), 427-436.
23. Svenson, S.; Tomalia, D. A., Dendrimers in biomedical applications—reflections on the field. *Advanced Drug Delivery Reviews* **2005,** *57* (15), 2106-2129.
24. Lombardo, D.; Calandra, P.; Bellocco, E.; Laganà, G.; Barreca, D.; Magazù, S.; Wanderlingh, U.; Kiselev, M. A., Effect of anionic and cationic polyamidoamine (PAMAM) dendrimers on a model lipid membrane. *Biochimica et Biophysica Acta (BBA)-Biomembranes* **2016,** *1858* (11), 2769-2777.
25. Gardikis, K.; Hatziantoniou, S.; Viras, K.; Wagner, M.; Demetzos, C., A DSC and Raman spectroscopy study on the effect of PAMAM dendrimer on DPPC model lipid membranes. *International journal of pharmaceutics* **2006,** *318* (1), 118-123.
26. Berényi, S.; Mihály, J.; Wacha, A.; Tőke, O.; Bóta, A., A mechanistic view of lipid membrane disrupting effect of PAMAM dendrimers. *Colloids and Surfaces B: Biointerfaces* **2014,** *118*, 164-171.
27. Åkesson, A.; Lind, T. K.; Barker, R.; Hughes, A.; Cárdenas, M., Unraveling dendrimer translocation across cell membrane mimics. *Langmuir* **2012,** *28* (36), 13025-13033.
28. Mecke, A.; Majoros, I. J.; Patri, A. K.; Baker, J. R.; Banaszak Holl, M. M.; Orr, B. G., Lipid bilayer disruption by polycationic polymers: the roles of size and chemical functional group. *Langmuir* **2005,** *21* (23), 10348-10354.
29. Lee, H.; Larson, R. G., Molecular dynamics simulations of PAMAM dendrimer-induced pore formation in DPPC bilayers with a coarse-grained model. *The Journal of Physical Chemistry B* **2006,** *110* (37), 18204-18211.
30. Lee, H.; Larson, R. G., Coarse-grained molecular dynamics studies of the concentration and size dependence of fifth-and seventh-generation PAMAM dendrimers on pore formation in DMPC bilayer. *The Journal of Physical Chemistry B* **2008,** *112* (26), 7778-7784.
31. Ma, Y.-q., pH-responsive dendrimers interacting with lipid membranes. *Soft Matter* **2012,** *8* (9), 2627-2632.

32. Marrink, S. J.; de Vries, A. H.; Mark, A. E., Coarse Grained Model for Semiquantitative Lipid Simulations. *The Journal of Physical Chemistry B* **2004,** *108* (2), 750-760.
33. Marrink, S. J.; Risselada, H. J.; Yefimov, S.; Tieleman, D. P.; de Vries, A. H., The MARTINI Force Field: Coarse Grained Model for Biomolecular Simulations. *The Journal of Physical Chemistry B* **2007,** *111* (27), 7812-7824.
34. Chong, L.; Dutt, M., Design of PAMAM-COO dendron-grafted surfaces to promote Pb(II) ion adsorption. *Phys Chem Chem Phys* **2015,** *17* (16), 10615-23.
35. Alder, B. J.; Wainwright, T. E., Studies in molecular dynamics. I. General method. *The Journal of Chemical Physics* **1959,** *31* (2), 459-466.
36. Allen, M. P.; Tildesley, D. J., *Computer simulation of liquids*. Oxford university press: 1989.
37. Frenkel, D.; Smit, B., *Understanding molecular simulation: from algorithms to applications*. Academic press: 2001; Vol. 1.
38. Plimpton, S., Fast parallel algorithms for short-range molecular dynamics. *Journal of computational physics* **1995,** *117* (1), 1-19.
39. Arnarez, C.; Uusitalo, J. J.; Masman, M. F.; Ingolfsson, H. I.; de Jong, D. H.; Melo, M. N.; Periole, X.; de Vries, A. H.; Marrink, S. J., Dry Martini, a coarse-grained force field for lipid membrane simulations with implicit solvent. *J Chem Theory Comput* **2015,** *11* (1), 260-75.
40. Wang, S.; Larson, R. G., Coarse-Grained molecular dynamics simulation of self-assembly and surface adsorption of ionic surfactants using an Implicit water model. *Langmuir* **2015,** *31* (4), 1262-1271.
41. Chong, L.; Aydin, F.; Dutt, M., Implicit solvent coarse-grained model of polyamidoamine dendrimers: Role of generation and pH. *J Comput Chem* **2016,** *37* (10), 920-6.
42. Wang, S.; Larson, R. G., A Coarse-Grained Implicit Solvent Model for Poly (ethylene oxide), Cn E m Surfactants, and Hydrophobically End-Capped Poly (ethylene oxide) and Its Application to Micelle Self-Assembly and Phase Behavior. *Macromolecules* **2015,** *48* (20), 7709-7718.
43. Wassenaar, T. A.; Ingólfsson, H. I.; Böckmann, R. A.; Tieleman, D. P.; Marrink, S. J., Computational Lipidomics with insane: A Versatile Tool for Generating Custom Membranes for Molecular Simulations. *Journal of Chemical Theory and Computation* **2015,** *11* (5), 2144-2155.
44. Feller, S. E.; Pastor, R. W., Constant surface tension simulations of lipid bilayers: the sensitivity of surface areas and compressibilities. *The Journal of chemical physics* **1999,** *111* (3), 1281-1287.
45. Lee, H.; Larson, R. G., Effects of PEGylation on the Size and Internal Structure of Dendrimers: Self-Penetration of Long PEG Chains into the Dendrimer Core. *Macromolecules* **2011,** *44* (7), 2291-2298.
46. Berendsen, H. J.; Postma, J. v.; van Gunsteren, W. F.; DiNola, A.; Haak, J., Molecular dynamics with coupling to an external bath. *The Journal of chemical physics* **1984,** *81* (8), 3684-3690.